

## RESEARCH ARTICLE

# Optimization of Polygonal Shaft Machining Parameters for Surface Roughness, Dimensional Error, and Cycle Time using Response Surface Methodology

U. Hanifah<sup>1</sup>, Novrinaldi<sup>1\*</sup>, M. Andrianto<sup>1</sup>, S. A. Putra<sup>1</sup>, A. Haryanto<sup>1</sup>, A. Taufan<sup>1</sup>, M. Furqon<sup>1</sup>, E. K. Pramono<sup>1</sup>, Y. H. Siregar<sup>2</sup>, D. Sagita<sup>1</sup>, Ma'muri<sup>1</sup>, M. Azka<sup>3</sup>, N. A. Rofik<sup>4</sup>, S. Rhamadhan<sup>5</sup>

<sup>1</sup>Research Center for Equipment Manufacturing Technology, National Research and Innovation Agency, 15314, Tangerang Selatan, Indonesia

<sup>2</sup>Research Center for Smart Mechatronics, National Research and Innovation Agency, 40135, Bandung, Indonesia

<sup>3</sup>Research Center for Manufacturing Technology of Production Machinery, 15314, Tangerang Selatan, Indonesia

<sup>4</sup>National Research and Innovation Agency, 15314, Tangerang Selatan, Banten, Indonesia

<sup>5</sup>Faculty of Engineering, Lampung University, 35141, Bandar Lampung, Indonesia

**ABSTRACT** – In power transmission, the shaft is a crucial component. During development, the cross-sectional features of the shaft are defined using specific geometric shapes, such as polygonal profiles, which require precision machining. This study examines the effects of machining parameters on surface roughness, dimensional accuracy, and machining time during the manufacture of polygonal shaft models made from AISI 304 and AISI 1020 materials. An experimental design, analysis, and optimization were employed using response surface methodology (RSM). Input parameters include cutting depth and cutting speed, while response parameters include surface roughness, dimensional error, and cycle time. Additionally, analysis of variance is used to determine the significance of input variables on response variables. The experiment began with a machining simulation in Esprit CAM software, followed by machining on a CNC Turn-mill machine. The workpiece was inspected using a surface roughness tester and a Coordinate Measuring Machine (CMM). The shortest machining time with the best machining quality per polygonal shaft standard was selected. Analysis of variance revealed that the input variables had a significant impact on surface roughness and cycle time ( $p$ -value  $< 0.0001$ ). However, they did not significantly affect dimensional error. The most influential parameter on the response of both materials was the depth of cut. AISI 304 material yields the best surface roughness value of  $0.3637\ \mu\text{m}$  at a cutting speed of 48 SPM and a depth of cut of 0.6 mm, while 1020 material yields  $0.4045\ \mu\text{m}$  at a cutting speed and depth of cut of 48 SPM and 0.6 mm. In contrast, 3.96 minutes and 5 minutes are the ideal machining times found for each material.

## ARTICLE HISTORY

Received : 27<sup>th</sup> Feb. 2025

Revised : 20<sup>th</sup> May 2025

Accepted : 14<sup>th</sup> Aug. 2025

Published : 16<sup>th</sup> Nov. 2025

## KEYWORDS

*Response surface methodology*

*Turn-milling*

*Polygonal shaft*

*Surface roughness*

*Dimension error*

*Time cycle*

## 1. INTRODUCTION

The isometric polygonal profile is a geometric representation of a polygon in isometric projection. In principle, this profile is a type of keyless connection that utilizes a non-circular cross-sectional shaft and a hub hole with the same profile [1]. In developing high-speed shafts, this profile is used in triangular, rectangular, hexagonal, and octagonal profiles as an alternative to the commonly used spline connections. The development of polygonal profile shafts is functionally intended for torque transmission with high transmission capacity [2] compared to conventional transmission. With an isometric profile, it can eliminate stress concentration or no additional stress with no pins between the shaft and hub [1][3][4], and the fatigue strength is higher than that of a spline connection [1][4]. The larger contact surface between the shaft and hub enables this connection to better balance rotating parts [5]. It is expected to reduce vibrations caused by rotation, making it very suitable for dynamic loads. Polygonal shafts are an excellent choice for connections that are frequently dismantled and reassembled. Economically, although it requires very tight manufacturing tolerances, production costs can be reduced by 40-50% compared to spline joints because the machining process is simpler, using a single machine and setup.

Several forms of shafts with polygonal profiles have been standardized by the German Standardization Institute (DIN), specifically for PC4 and P3 shafts, where the corresponding size specifies their use. Several machining methods have been applied to the manufacture of polygonal profiles, including computer-based numerical control (CNC) grinding [5] and NC Grinding [6][7], with the addition of tool accessories that employ eccentric mechanisms. Harmonious movements on the x and y axes, and the relationship between the two is proportional transmission. Szabó [8] used an eccentric mechanism grinding machine to shape polygonal profiles by applying it to the chisel's geometry. Maximov [9] conducted a finite element simulation and kinematic synthesis. This mechanical engineering process designs the size and configuration of the mechanism to achieve the desired motion in machining hypocycloidal polygon shaft joints. Machining motion engineering is applied on a lathe. Arndt et al. [2] discussed tool modeling for the machining of

\*CORRESPONDING AUTHOR | Novrinaldi | ✉ [novr002@brin.go.id](mailto:novr002@brin.go.id)

polygonal internal profiles, which was validated experimentally. Modeling and experiments focused on hypocycloidal internal profiles using a numerical approach based on the Dixel model and on machining using an alternative drive system on a lathe. Soliman [10] conducted simulation-based modeling to consider the kinematic parameters and dimensions of the turning process. The simulation examines the impact of the speed ratio and the number of cutting inserts on the shape of the cross-sectional profile, including its associated errors. The milling process has also been employed in manufacturing polygonal profiles using Universal CNC lathes by Regus et al. [11]. The formation of polygons (polygon shaping) using the plain milling and face milling methods involves synchronizing spindle movement and tool rotation.

In industrial processes, metal forming is often performed by cutting, which removes unwanted material [12]. This process is part of the manufacturing process used to transform raw materials into the desired end product by changing their shape and size. In its development, the manufacturing process has undergone a significant transformation from conventional to modern machining technology. The machining process, which was previously dominated by operator skill with simple tools, was low-precision, time-consuming, and error-prone. It has been replaced by modern machining technology that can eliminate all these shortcomings. Modern machining technology often integrates CNC to ensure high precision, consistency, and production efficiency. This machining process yields a component with tolerances and surface quality that meet the technical specifications.

Surface quality is a crucial element of an automated production process, one of the most important criteria in the metal cutting area [13], and a key technical indicator for measuring the surface quality of parts [14]. Surface quality has a direct impact on several key aspects of the manufacturing process, including product precision and accuracy, efficiency and productivity, wear and tool life, costs, and safety considerations. Therefore, surface quality can be used as an objective function in an optimization process. One surface quality parameter is surface roughness. This parameter is crucial for evaluating the quality of a machined surface because it affects the final product's performance, functionality, and aesthetics. Surface roughness refers to the texture of a machined surface and is characterized by arithmetic average roughness ( $R_a$ ) and ten-point height of irregularities ( $R_z$ ) parameters.  $R_a$  is the average absolute value of the surface height deviation measured from the mean line at a certain length. This parameter is commonly used in industry to measure surface roughness. On the contrary,  $R_z$  indicates the average of the absolute values of the five highest peaks and the depths of the five deepest valleys in the sampling length [15]. Roy et al. [16] discussed cutting tool failures that affect the surface quality of AISI 4340 steel during turning using the pulsating MQL (Pu-MQL) cooling method. This research demonstrates that machining parameters, including feed, cutting speed, and depth of cut, significantly impact cutting tool wear, while cutting tool conditions substantially influence the surface quality of the machined workpiece. The MQL pulsating cooling method ensures the cutting tool remains in optimal condition. This method of supplying lubricant to the cutting area with a pulse mode can minimize cutting tool wear and workpiece surface roughness. Anurag et al. [17] compared three machining conditions of the Titanium alloy Ti-6Al-4V ELI, namely dry conditions, MQL (minimum quantity lubrication), and SIC (spray impingement cooling), to analyze tool wear, surface roughness, surface topology, cutting temperature, and chip morphology.

The research results show that cutting conditions with the MQL method result in lower wear and surface roughness than the other two conditions; thus, this method can indirectly help reduce the biological and ecological impacts of the machining process. The MQL method also has a longer tool life, 177.77% greater than the dry and SIC methods, and is estimated to reach 1500 seconds. The optimal conditions for the turning process of Titanium alloy Ti-6Al-4V ELI are MQL with a depth of cut of 0.2 mm, a feed rate of 0.12 mm/revolution, and a cutting speed of 79 m/minute. Optimization of the objective function in the form of surface roughness was also carried out by Najiha et al. [18], who used 6061-T6 aluminum alloy in the end-milling process, combined with MQL lubrication using a  $TiO_2$ -based nanofluid. The optimized machining parameters were cutting speed, feed rate, depth of cut, MQL flow rate, and nanofluid volume concentration. This research demonstrates that the Pareto frontier solution, with the following parameter configuration: cutting speed of 5427.4 RPM, feed rate of 342.55 mm/min, depth of cut of 2.895 mm, MQL flow rate of 0.31 mL/min, and nanofluid volume concentration of 1.43%, represents the optimal setup for achieving the desired optimization objectives.

In other studies, various methods have been developed to predict and monitor surface roughness during machining, underscoring the importance of CNC machining outcomes for quality and efficiency. Ruilin Liu & Wenwen Tian [14] developed a new two-task simultaneous monitoring method for surface roughness and tool wear, which was then verified through end-face milling experiments using a vertical machining center. This method, called the Broad Echo State Two-Task Learning System (BESTTLS), is designed to capture the dynamic characteristics of each subtask. In the verification process, vibration, current, and cutting force signals were collected, followed by feature extraction and nonlinear dimensionality reduction. The results indicate that BESTTLS significantly outperforms the other methods in simultaneously monitoring surface roughness and tool wear. Trinh [13] developed a method for predicting surface roughness in machining. This model is based on cutting theory, experimental investigation methods, artificial intelligence methods, and experimental design methods. Li et al [19] discussed the quality and prediction of surface roughness in turning. The mechanisms of tool wear and cutting vibration were analyzed to predict surface roughness and improve machining quality. In the turning experiment, the machining parameters used were Cutting Depth, Feed Rate, Cutting Speed, Spindle Speed, and Workpiece diameter. This experiment revealed that spindle diameter is an important factor that affects the amplitude and frequency of vibration. The prediction results show that surface roughness increases with increasing tool wear and decreases with increasing workpiece diameter.

The optimization of machining using various techniques in turning or milling processes has been widely discussed in previous studies. Kumar et al. [20] used Taguchi and Grey Relational Analysis (GRA) to optimize the process parameters during the machining of 304 stainless steel (SS 304) using an end mill. Experimental research was done on four primary machining input parameters: feed rate, coolant presence or absence, and cutting speed. Surface roughness, surface strain, and microhardness were the response parameters that were examined. This study indicates that the ideal conditions for SS 304 end milling are with the coolant system active, feed rates of 2500 mm/min, cutting depths of 0.4 mm, and cutting speeds of 1500 rpm. Additionally, the results indicated that cutting speed accounted for 26% of the overall process, indicating it is the parameter with the highest contribution. In the milling machining of magnesium alloy AZ91, Verma et al [21] also performed additional machining optimization using the Taguchi method. ANOVA analysis revealed that the optimal machining parameters are a cutting speed of 3000 rpm, a depth of cut of 0.5 mm, a feed rate of 150 mm/min, and a surface roughness of 0.22  $\mu\text{m}$ . Additionally, it was concluded that feed rate is the most important determinant of surface quality.

Mahesh and Rajesh [22] optimized the cutting parameters (depth, feed, and cutting speed) and the nose radius for processing Al 7075-T6 using the Taguchi method. Using ANOVA, they found that the nose radius and depth of cut have a considerable effect on surface roughness, accounting for at least 31% of the total variation. Nisar et al. [23] examined the effects of feed rate, spindle speed, and depth of cut on the milling process of copper X3Y1Z1 material on product quality, including dimensional accuracy and surface finish. Optimal parameters were optimized and combined using the GRA and the Taguchi method orthogonal array. ANOVA analysis showed that feed rate had a significant impact on surface roughness and dimensional accuracy. The following parameters contributed significantly: depth of cut and spindle speed.

The Taguchi method has also been applied to optimize the turning and milling processes. To achieve the lowest possible final surface quality, Villeta et al. [24] dry turned magnesium while controlling for feed rate, cutting speed, and tool coatings. The most important determinant of optimal surface quality is feed rate. For an average roughness of 0.306  $\mu\text{m}$  and 0.406  $\mu\text{m}$ , the best parameter combination was found in two combinations of cutting speed, feed rate, and tool coatings parameters: 150 m/min–0.05 mm/rev–HX, 225 m/min–0.05 mm/rev–HX, 150 m/min–0.05 mm/rev–TP200, and 225 m/min–0.05 mm/rev–TK2000. The Taguchi method was also employed by Kumar et al. [25] to optimize surface roughness in the machining of a titanium composite. Ayyildiz [26] optimization and prediction of surface roughness in the milling process of aluminum alloy using the Taguchi method and artificial neural network. Ayyildiz [26] combined the Taguchi method and artificial neural network (ANN) to optimize and predict surface roughness in the milling process of aluminum alloy using cryogenically and non-cryogenically treated cutting tools. This study concluded that the Taguchi method effectively optimized the machining parameters, and the artificial neural network model demonstrated strong predictive accuracy, confirming its suitability for estimating surface roughness in the milling process. Feed rate was the most significant machining parameter affecting surface quality.

Sarkaya and Güllü [27] combined Taguchi design with Response Surface Methodology (RSM) to optimize the machining parameters of the AISI 1050 turning process. ANOVA analysis revealed that feed rate significantly improves surface quality in cutting operations, with the greatest impact on cooling conditions, surface roughness, and minimum quantity lubrication (MQL). Kumar and Meenu [28] optimized additional machining parameters for turning unidirectional glass fiber-reinforced plastic composite (UD-GFRP). To reduce surface roughness and increase the rate of material removal, Taguchi and ANOVA techniques, as well as GRA, were applied to analyze the following parameters: depth of cut, feed, tool rake angle, speed, cutting environment, and tool nose radius. The machining zone was flooded with a miscible soluble coolant and Castrol water (1:6). The experiment was conducted in a cold ( $5^{\circ}$ – $7^{\circ}\text{C}$ ) and wet ( $33^{\circ}$ – $38^{\circ}\text{C}$ ) cutting environment. The primary determinants of minimum surface roughness (1,761  $\mu\text{m}$ ) and maximum material removal rate (275.8  $\text{mm}^3$ ) are cutting speed and feed rate, respectively. Environmentally friendly turning machining was studied by Singh et al. [29] to reduce the adverse effects of cutting fluids on both the environment and operators. PVD-coated carbide tools were used in dry, flooded, and nanofluid minimum quantity lubrication (NF-MQL) tests on AISI 304 material. Using nanofluid cutting fluid (NF-MQL), the optimal parameters to achieve a surface roughness of 0.509  $\mu\text{m}$  and tool wear of 100.001  $\mu\text{m}$  were determined as a depth of cut of 0.25 mm, a feed of 0.06 mm/rev, and a cutting speed of 160.67 m/min.

Mugendiran et al. [30] optimized machining parameters, such as spindle speed, feed rate, and step size, by employing RSM to improve the surface roughness and wall thickness of AA5052 aluminum. Furthermore, Roy et al. [31] employed RSM to examine how critical milling machining parameters, such as feed rate, depth of cut, and spindle speed, affect minimum surface roughness. Minimum feed rate, maximum spindle speed, and depth of cut result in the workpiece's final surface having the least amount of surface roughness. The RSM method was applied by Puoza et al [32] to determine the ideal turning process parameters. Thirteen experiments were conducted on AL6061 material using a Slant Bed Turning/Center/Computer Numerical Control (SB/C/CNC) precision lathe. Cutting speed and feed rate were among the optimized parameters to assess surface roughness, dimensional error, and microhardness. According to the evaluation results, the maximum surface microhardness was generated at a feed rate of 0.231 mm/rev and a cutting speed of 154.363 m/min. A cutting speed of 154.363 m/min and feed rates of 0.1389 mm/rev, 152.081 m/min, and 0.1025 mm/rev, respectively, resulted in the lowest dimensional error and surface roughness.

This study examines the impact of operational factors, specifically cutting parameters, including cutting speed and depth of cut, on surface roughness (Ra), dimensional error, and time cycle. These parameters are applied experimentally to the turn-milling process in manufacturing polygonal shaft models using AISI 304 and AISI 1020 materials. Furthermore, the optimal machining parameters are determined using the Response Surface Methodology.

## 2. METHODS AND MATERIAL

### 2.1 Experimental Set-up and Procedure

In this study, a polygonal profile shaft model was employed, with stainless steel and carbon steel as the two materials. The two materials are comparable to AISI 304 and AISI 1020, as defined by the American Iron and Steel Institute (AISI) standards. This type of material is easy to obtain and relatively cheap and easy to fabricate, so it is widely used in the food and beverage industry (dairy processing industry, food mixers), chemical and pharmaceutical industries (chemical storage tanks, reactors, boiler tubing [33]) pipes, valves), manufacturing and machinery (shafts), and pipes and fluid systems. The mechanical characteristics of the materials under investigation are displayed in Table 1. These two materials are also frequently used in the production of machine parts, and their characteristics influence the machining process and quality. The rough workpiece used in this study had dimensions of 50 mm in length and 30 mm in diameter. Later, the workpiece's diameter was reduced to 25 mm, based on the polygonal profile's largest diameter.

Table 1. Properties of stainless steel AISI 304 and carbon steel AISI 1020

Properties	Units	Material	
		AISI 304	AISI 1020 (at T 25°C)
Density	kg/m <sup>3</sup>	8000	7700- 8030
Hardness	HRD	11.6	33.3
Ultimate Tensile Strength	Mpa	505	394.7
Yield Tensile Strength	Mpa	215	294.8
Elastic Modulus	GPa	193	190-210
Shear Modulus	GPa	77	80
Thermal Conductivity	W/m.K	16.2 (at 0-100 °C)	51.9

Source: matweb.com

As shown in Figure 1, the manufacturing process for the polygonal shaft profiles used in this study involves multiple steps, including design preparation, toolpath simulation, machining, and inspection measurement. Initially, SolidWorks 2021 was used to model the profile. The end product is a 3D shape that can be utilized for precision machining and machining process planning [34]. Second, to save time and cost, the toolpath topology and machining process are determined using CAM software (Esprit 20210) simulation. By displaying machining process details, CAM visualization helps to produce precise products and foresee safety-related hazards. The NC code used for the CNC machining process was the outcome of this step.

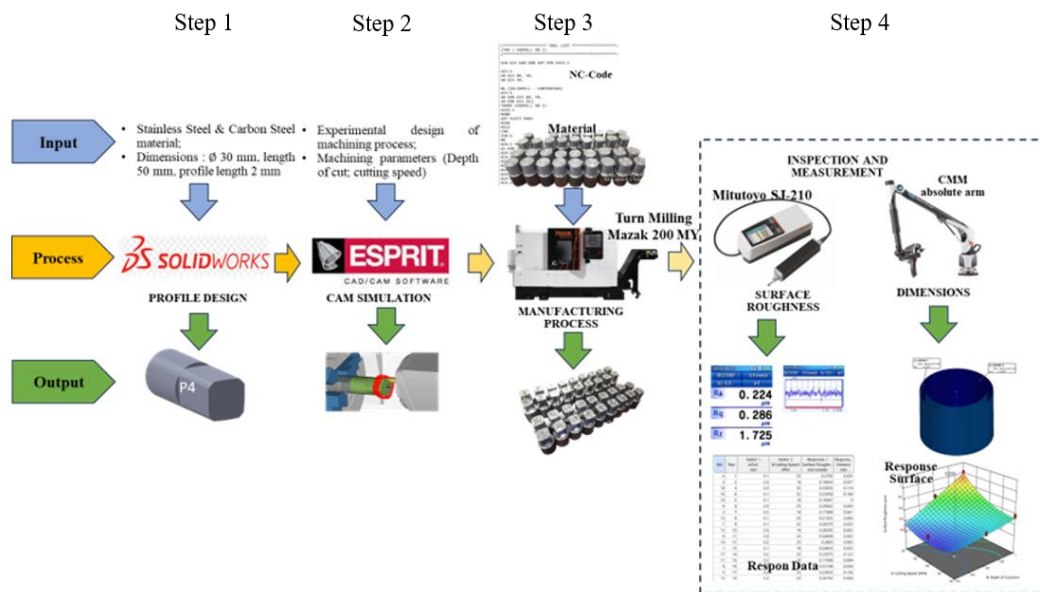


Figure 1. Schematic diagram of experimental set-up

Furthermore, the design of experiment was used to identify the parameter combinations, which are covered in more detail in the subsection that follows. Eighteen workpieces were produced in the next step, which involved machining each experimental combination using a CNC turn-milling machine (Mazak QTE-200MY SG). All workpieces are subsequently examined and measured for additional dimensions and roughness analysis.

Furthermore, the experiment's design was used to identify the parameter combinations, which are covered in more detail in the subsection that follows. A coaxial turn-milling process with a chain-machining strategy is used. A carbide end mill type with three flutes and an 8 mm diameter was used to feed the workpiece. The workpiece axis and the tool axis rotate about their respective axes at the same time. The axial direction of the cutter's (tool's) z-axis, which runs parallel to the workpiece axis, is the depth of cut.

**2.2 Optimization using Response Surface Methodology**

To determine the optimal conditions for the machining process, a design of experiments methodology was employed to plan the experiments and analyze the data. Cutting speed (SPM) and depth of cut (mm) are two machining parameters that are displayed in Table 2 along with the level of each component. Additionally, the response surface methodology (RSM) will be used to analyze the relationships between the response variables and the independent variables (factors). Additionally, the significance of the parameters that form the response variables is examined using variance analysis (ANOVA).

Additionally, the forming parameters that significantly impact Ra, dimensional error, and time cycle are examined using a post hoc analysis. By examining the intended response in terms of surface quality and minimizing errors in the workpiece's dimensions while achieving the intended minimum machining time, the machining process is optimized through the interaction of these two factors. Eighteen tests of the factors and levels used, with two repetitions, were generated by the RSM experimental design. In addition, the experimental design parameters were incorporated into the CAM simulation procedure.

Table 2. Machining parameters for Stainless Steel and Carbon Steel material

Stainless steel AISI 304 and carbon steel AISI 1020			
Faktor		Level	
A	<i>Cutting Speed (CS)</i> (SPM)	LA1	32
		LA2	48
		LA3	64
B	<i>Depth of Cut (DoC)</i> (mm)	LB1	0.2
		LB2	0.6
		LB3	1.0

Table 3. Constraints for factors and response optimization of polygonal shaft model machining process with AISI 304 and AISI 1020 materials using RSM

Name	Goal	Limit		Weight		Importance
		Lower	Upper	Lower	Upper	
AISI 304						
Cutting Speed (A)	within the range	32	64	1	1	3
Depth of Cut (B)	within the range	0.2	1	1	1	3
Surface Roughness	minimize	0.4	1	1	1	5
Dimensions Error	minimize	-0.02	0.015	1	1	5
Time Cycle	within the range	2.5	5	1	1	3
AISI 1020						
Cutting Speed (A)	within the range	32	64	1	1	3
Depth of Cut (B)	within the range	0.2	1	1	1	3
Surface Roughness	minimize	0.4	1	1	1	5
Dimensions Error	minimize	-0.02	0.015	1	1	5
Time Cycle	within the range	2	5	1	1	3

The input and output variables are constrained in order to achieve the best possible results during the machining process. In order to produce the appropriate solution based on the actual conditions required for the desired machining results, the combination of input variables and their constraints will be crucial. As indicated in Table 3, the cutting speed, depth of cut, and time cycle limit inputs are preset. However, as their constraints, the response variables—such as dimension error and surface roughness—are minimized while remaining within their respective standard ranges. G6 and

K6 shaft fit transitions with a surface roughness range of 0.4-1.6  $\mu\text{m}$  and a range of (-)20 to (+)15  $\mu\text{m}$  are used for dimensional tolerances in accordance with DIN 37212 for shaft diameters of 25 mm.

A four-axis CNC turn-milling machine was used to machine the polygonal profile model along 20 mm of the material's overall length. A chain-machining approach is combined with a coaxial turn-milling process. A carbide end mill-style tool with three flutes and an 8 mm diameter is used to feed the workpiece. The workpiece axis and the tool axis rotate about their respective axes at the same time. The axial direction of the cutter's (tool's) z-axis parallel to the workpiece axis is known as the depth of cut.

### 2.3 Inspection and Measurement

#### 2.3.1 Surface roughness

Surface quality is a crucial aspect of the manufacturing process, influencing several key final product characteristics. Surface quality encompasses the physical properties of a material's surface, including waviness, surface roughness, flaws, and lay. Surface roughness refers to small and subtle deviations or unevenness from a nominal surface determined by the characteristics of the materials and processes that form that surface [35]. This surface roughness is measured by observing minor variations in an object's surface, such as peaks or valleys, on a micron scale or smaller. The greater the deviation from the actual shape, the rougher the surface, the smaller the deviation, the smoother the surface. Several factors influence surface roughness and contribute to achieving the desired quality. However, in general, they are categorized into three main groups, namely set-up factors such as machine tool, workpiece and cutting tool factors [12] operation factors in the form of cutting parameters like depth of cut, feed rate and cutting speed [36], [37], [38] and process parameters (cutting strategies, coolant) and processing factors such as tool wear, vibration, etc. [39] with several factors that have a direct influence on surface quality.

Surface roughness measurements can be performed using three methods: optical techniques, electronic stylus instruments and subjective comparisons with standard test surfaces [35]. Surface quality measurements follow ISO 4287:1997, which outlines methods for evaluating and measuring surface quality along linear profiles on specific lines on the material. Surface roughness measurement using electronic stylus instruments employs a direct-contact method between the stylus and the measured object. The probe (pick-up) moves horizontally along the surface to be measured with a stylus, and the stylus, which moves vertically, adjusts to the surface profile being measured to obtain deviations in the form of a surface profile [40] [41] (Figure 2).

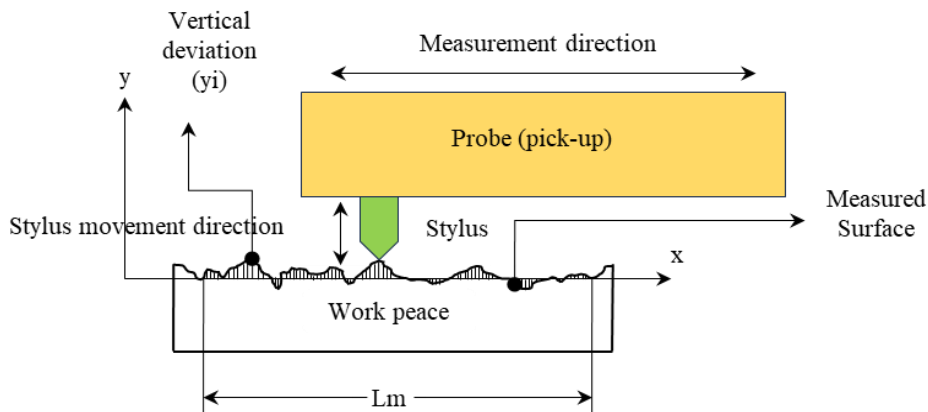


Figure 2. Illustration of surface roughness measurement using a stylus-type instrument

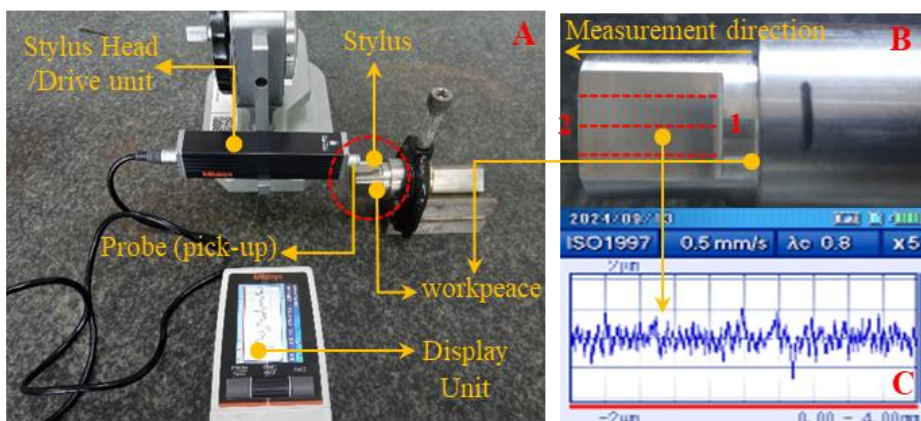


Figure 3. (a) Stylus-type instrument for measuring surface roughness, (b) measured point, (c) photographic result of surface roughness measurement

Figure 3(a) illustrates the measurement scheme for surface roughness using the Mitutoyo SJ210 stylus electronic instrument method, which comprises two main components: the drive unit (stylus head, probe, and stylus) and the display unit. Measurements were carried out on the four sides of the machined polygonal profile. Three passes were measured on each side, and the overall surface roughness was determined as the average of these values (Figure 3(b)). The stylus on the drive unit or measuring needle moves linearly from point 1 to point 2, and differences or variations in the height of the measured object's surface will cause the stylus to move vertically following its roughness. The results of surface roughness measurements are presented in either numerical or graphical form, showing the polygonal profile's surface topography (Figure 3(c)). The measurement data are the arithmetic average roughness ( $R_a$ ) and peak-lowest roughness ( $R_z$ ). Surface roughness can be defined as the average vertical deviation ( $y_i$ ) (Figure 2) from the nominal surface at a particular surface length ( $L_m$ ) (Figure 2) [34]. The average surface roughness in the form of the arithmetic average is defined in the form of the following equation:

$$R_a = \int_0^{L_m} \frac{|y|}{L_m} dx \quad (1)$$

Surface roughness is the average of the vertical distance deviations of a nominal surface over a specified surface length. The average roughness refers to the arithmetic average of the absolute values of the deviations.

### 2.3.2 Dimensions

The final dimensions of a workpiece are highly dependent on various internal factors, including machine rigidity and stability, material properties, tool wear, and machining parameters. The difference between the measured and designed dimensions is known as dimensional error. To ensure components meet the required specifications, dimensional control is performed through measurements and inspections. In the meantime, environmental, lubricating, and cooling factors are examples of external factors. The kinematic movements of the milling process, such as linear, rotational, and multi-axis motion, also have a significant impact on dimensions, particularly when vibrations increase.

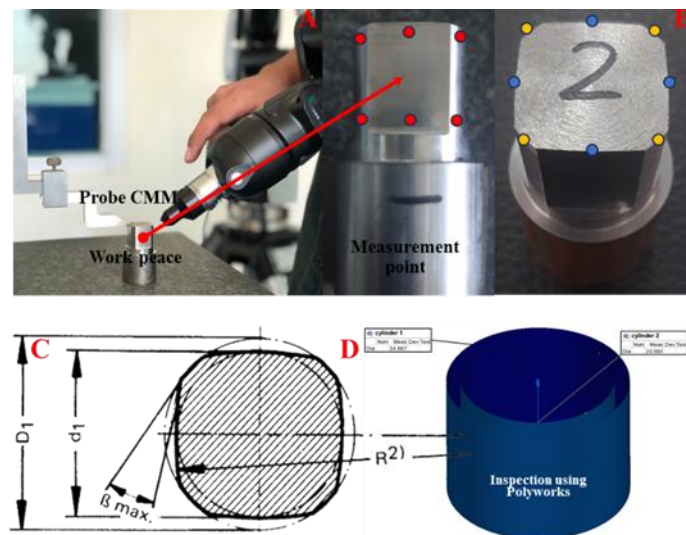


Figure 4. (a) Dimensional measurement method using CMM absolute arm using the probe, (b) Top view: dimension measurement points, (c) Basic dimensions of polygonal profile, (d) Dimensional inspection using PolyWorks Inspector software

An absolute-arm-type coordinate measuring machine (CMM) (Figure 4(a)) is used in this study to measure the dimensions of the machined parts. Polyworks software is used to process the measurement data. The dimensions of the machining results are measured at preset points using the CMM's probe (Figure 4(b)). Figure 4 (c) illustrates how the dimensions of the workpiece to be measured are determined by the size of the cylinders, which form the foundation of the polygonal profile model. These cylinders are the tiny cylinder ( $d_1$ ) and the large cylinder ( $D_1$ ). On the other hand, Figure 4(b) displays the workpiece machining results for the smallest and largest diameters, represented by blue and yellow dots, respectively. Measurements at eight points for each cylinder were analyzed in Polyworks to determine the dimensions of the two cylinders (Figure 4(c)). Both have design dimensions of 21 mm and 25 mm, respectively.

### 2.3.3 Time Cycle

In the machining process, time is crucial, as it significantly affects production efficiency. To make their products more competitive, producers can significantly benefit from effective time management in the production process. The machine and tools used, the material properties, the type of machining process, the machining parameters, and the complexity of the geometry to be processed are some of the factors that affect production time. Among these, the correct machining approach is essential to ensure high-quality, efficient machining.

### 3. RESULTS AND DISCUSSION

Table 4 shows the 18 combinations, as was indicated in the preceding section. Additionally, following the simulation and/or machining process, the table displays the RA, DE, and TC results. AISI 304 exhibits the lowest Ra, DE, and TC of 0.2424  $\mu\text{m}$ , 0.1000 mm, and 2.47 minutes, respectively. The CS/DoC combinations for each of the previously mentioned highest values are 32 SPM/0.2 mm, 64 SPM/0.2 mm, and 32 SPM/0.2 mm, respectively. According to AISI 1020, the lowest values of Ra, DE, and TC are 0.1731  $\mu\text{m}$ , -0.1660 mm, and 1.93 minutes, respectively.

The CS/DoC combinations for each of the highest values previously mentioned are 32 SPM/0.2 mm, 48 SPM/1 mm, and 64 SPM/1 mm, respectively. The ensuing sections will also present additional analysis to maximize the trade-off between the results.

Table 4. Data response surface of the experiment and results

Run	AISI 304					AISI 1020				
	CS (SPM)	DoC (mm)	Ra ( $\mu\text{m}$ )	DE (mm)	TC (minutes)	CS (SPM)	DoC (mm)	Ra ( $\mu\text{m}$ )	DE (mm)	TC (minutes)
1	48	0.6	0.3823	0.0085	3.78	48	0.2	0.3335	-0.0600	10.00
2	64	0.2	0.2799	-0.1000	7.92	48	0.6	0.4978	-0.0185	3.67
3	32	0.6	0.7165	-0.0590	5.10	32	1	0.8415	-0.0205	3.62
4	64	0.2	0.2678	-0.0180	8.53	32	0.2	0.1731	-0.1220	15.75
5	64	0.6	0.4228	-0.0165	3.08	64	0.2	0.2855	-0.0340	7.97
6	32	0.2	0.2424	0.0170	21.08	32	1.0	0.9745	0.0245	3.62
7	32	0.2	0.3143	-0.0385	21.08	64	1.0	0.5805	0.0110	1.93
8	64	1.0	0.5807	0.0245	2.47	48	0.2	0.3785	0.0410	10.00
9	32	0.6	0.6858	-0.0175	5.10	48	0.6	0.4896	-0.0420	3.67
10	48	1.0	0.5183	-0.0430	2.88	64	1.0	0.5195	-0.0415	1.93
11	32	1.0	1.0178	-0.0430	4.00	48	1.0	0.5121	-0.0405	2.47
12	32	1.0	1.0312	0.0130	4.00	64	0.2	0.3099	-0.0055	7.97
13	48	0.6	0.3162	-0.0290	3.78	32	0.6	0.6048	-0.0520	5.57
14	48	1.0	0.5926	-0.0775	2.88	32	0.6	0.7594	-0.0485	5.57
15	64	0.6	0.4650	0.0225	3.28	64	0.6	0.4863	-0.0375	3.17
16	48	0.2	0.3783	-0.0125	10.58	64	0.6	0.4877	-0.0980	3.17
17	64	1.0	0.5428	-0.0120	2.47	32	0.2	0.2785	-0.0405	15.75
18	48	0.2	0.3376	-0.0150	10.55	48	1.0	0.4490	-0.1660	2.47

Note: CS: cutting speed, DoC: depth of cut, Ra: surface roughness, DE: dimensions error, TC: time cycle

#### 3.1 Statistical Analysis of Surface Roughness (Ra)

According to Khorasani et al. [42], the six primary categories that affect surface roughness are cutting parameters, dynamic parameters, thermal parameters, workpiece properties, machine tool properties, and tool properties. The quality of the surface roughness of the machining results is significantly influenced by the machining parameters, which are an independent factor in the optimization process. Surface quality has been the subject of numerous studies, making it a technological parameter that needs to be continuously improved [43] while cutting costs by minimizing time [42]. Cutting speed (A) and depth of cut (B) are input factors in this study that are optimized to produce the best possible response (output). Optimal response surface methodology was employed to model and analyze the ideal conditions for achieving the lowest surface roughness in AISI 304 and AISI 1020 materials.

The ANOVA response quadratic model for AISI 304 and 1020 is summarized in Table 5 in order to assess how the depth of cut (B) and cutting speed (A) factors affect the surface roughness response. The F probability value with a 95% confidence level was used to evaluate the model [30]. The model and its terms were statistically significant when the P values were less than 0.05 [24]. A very significant model explaining changes in the input variables in the desired response variable is the AISI 304 Model, as indicated by its F-value of 20.85 (p-value < 0.0001).

The variable with the greatest contribution (very significant,  $p < 0.0001$ ) to the response is depth of cut (B), with an F-value of 62.02; cutting speed (A) has an F-value of 21.46 ( $p = 0.0006$ ). The F-values of 12.88 ( $p = 0.0037$ ) and 7.84 ( $p = 0.0161$ ) indicate that the interaction of factors A and B (AB) and A2 also contributed significantly. B2 had no discernible effect on the model ( $p = 0.8192$ ; F-value = 0.0546). The coefficient of determination ( $R^2$ ), which ranges from 0 to 1, indicates the quality of the statistical model; a value close to 1 is ideal [30]. The Adjusted  $R^2$  of 0.8538 and the predicted  $R^2$  of 0.7756 are in agreement.

The model is significant for AISI 1020, as indicated by an F-value of 12.85 ( $p = 0.0002, p < 0.05$ ). In the quadratic model for surface roughness response, the depth of cut (B) factor contributes the most, with an F-value of 40.12 ( $P < 0.0001$ ), followed by the cutting speed F-value of 8.28 ( $p = 0.0139$ ), just like in AISI 304. Additionally, with an F-value of 9.92 ( $p = 0.0084$ ), the interaction between A and B contributes significantly. The model was not significantly impacted by quadratic terms A2 or B2, as indicated by their respective F-values of 2.87 ( $p = 0.1163$ ) and 3.07 ( $p = 0.1052$ ). The Adjusted  $R^2$  of 0.7771 and the Predicted  $R^2$  of 0.6443 demonstrate the quality of the statistical model.

In the industry, surface roughness modeling is considered a primary tool for optimizing parameters that improve surface quality [44]. The quadratic regression model equation for predicting surface roughness resulting from the interaction of the independent variables cutting speed (A) and depth of cut (B) for AISI 304 and 1020 materials is displayed in Equations (2) and (3). The coefficients have respective positive and negative values. Every variable displays the impact of both rising and falling surface roughness levels.

$$\{Ra(AISI\ 304) = 1.11390 - 0.044201 \cdot CS + 1.29314 \cdot DoC - 0.017899 \cdot CS \cdot DoC + 0.000494 \cdot CS^2 + 0.065935 \cdot DoC^2\} R^2 = 89.68\%, R_{Adj}^2 = 85.38\% \tag{2}$$

$$\{Ra(AISI\ 1020) = 0.536963 - 0.025574 \cdot CS + 1.88179 \cdot DoC - 0.016794 \cdot CS \cdot DoC + 0.000319 \cdot CS^2 - 0.528691 \cdot DoC^2\} R^2 = 84.26\%, R_{Adj}^2 = 77.71\% \tag{3}$$

Several factors influence surface roughness. They are tool side wear and setup factors, such as the workpiece [45]. Cutting parameters [46] and processing factors such as vibrations [47], [48], [49], [50] and tool wear [51], [45] are examples of operational factors.

Table 5. ANOVA for Response Quadratic Model (response: Surface roughness (Ra) in  $\mu m$ )

Source	Sum of Squares	df	Mean Square	F-value	p-value	
AISI 304						
Model	0.8498	5	0.1700	20.85	< 0.0001	significant
Cutting Speed (A)	0.1749	1	0.1749	21.46	0.0006	
Depth of Cut (B)	0.5055	1	0.5055	62.02	< 0.0001	
AB	0.1050	1	0.1050	12.88	0.0037	
A <sup>2</sup>	0.0639	1	0.0639	7.84	0.0161	
B <sup>2</sup>	0.0004	1	0.0004	0.0546	0.8192	
Residual	0.0978	12	0.0082			
Lack of Fit	0.0872	3	0.0291	24.70	0.0001	significant
Pure Error	0.0106	9	0.0012			
Cor Total	0.9476	17				
Standard Deviation	0.0903		R <sup>2</sup>	0.8968		
Mean	0.5051		Adjusted R <sup>2</sup>	0.8538		
C.V. %	17.87		Predicted R <sup>2</sup>	0.7756		
PRESS	0.2127		Adeq. Precision	14.8140		
AISI 1020						
Model	0.5988	5	0.1198	12.85	0.0002	significant
A-Cutting Speed	0.0772	1	0.0772	8.28	0.0139	
B-Depth of Cut	0.3739	1	0.3739	40.12	< 0.0001	
AB	0.0924	1	0.0924	9.92	0.0084	
A <sup>2</sup>	0.0267	1	0.0267	2.87	0.1163	
B <sup>2</sup>	0.0286	1	0.0286	3.07	0.1052	
Residual	0.1118	12	0.0093			
Lack of Fit	0.0803	3	0.0268	7.63	0.0076	significant
Pure Error	0.0315	9	0.0035			
Cor Total	0.7106	17				
Standard Deviation	0.0965		R <sup>2</sup>	0.8426		
Mean	0.4979		Adjusted R <sup>2</sup>	0.7771		
C.V. %	19.39		Predicted R <sup>2</sup>	0.6443		
PRESS	0.2527		Adeq. Precision	11.1675		

The 3D response surface interaction between two input variables (depth of cut (B) and cutting speed (A)) on the response [27] surface roughness (Ra) is shown in Figure 5, along with the regression equation in graphical form. The contour lines in Figures 5(a) and 5(b) on the XY plane illustrate how the surface roughness value changes for AISI 304 and AISI 1020 materials in relation to cutting speed and depth of cut. To determine the ideal value of the intended

maximum or minimum response, plot the interaction of the two input variables mentioned above. Low surface roughness is typically the result of the interaction between a low depth of cut ( $\pm 0.2$  mm) and a high cutting speed ( $\pm 64$  SPM).

Low cutting speeds and cut depths increase surface roughness. According to Figure 5(a), this demonstrates that increasing the depth of cut considerably increases surface roughness [52],[53], thereby lowering the workpiece's surface quality after the machining process. For improved surface quality, low depth of cut and high cutting speed are required. In their explanation of this technique, Nisar et al [23] report that the milling machining process yields the best surface quality at the lowest depth of cut, 0.1 mm. At a cutting speed of 48 SPM and a depth of cut of 0.6 mm, the optimization results yielded a surface roughness of  $0.3637\mu\text{m}$ . This outcome remains within the acceptable range of surface roughness for the PC4 transition fit polygonal shaft's surface quality (g6 or k6).

The surface roughness of workpieces made from AISI 1020 material illustrates how input variables interact with output response variables, as shown in Figure 5(b). The response characteristics are generally the same as those of AISI 304 material, where surface roughness tends to increase or become rougher with increasing depth of cut and decrease with increasing cutting speed. The interaction between machining parameters results in a decrease in workpiece surface quality, as indicated by the increase in surface roughness for these two materials [54]. According to the optimization results, the depth of cut was 0.6 mm, and the cutting speed was 48 SPM, resulting in a surface roughness of  $0.4045\mu\text{m}$ .

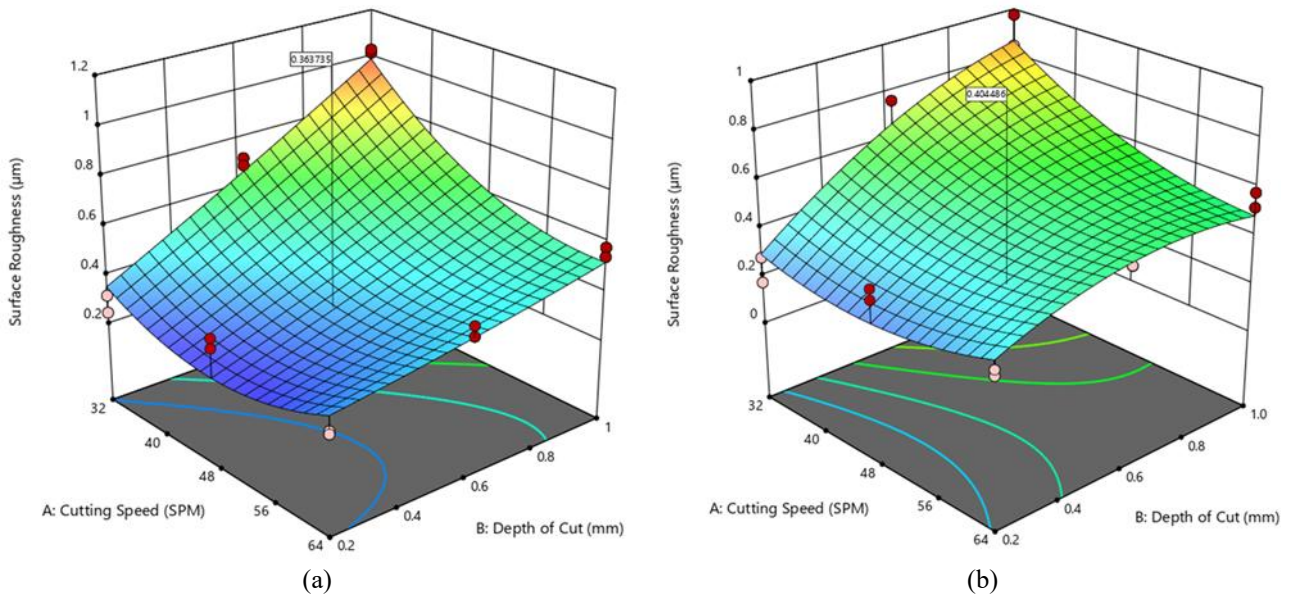


Figure 5. 3D response surface plot for surface roughness (Ra) of (a) AISI 304 and (b) AISI 1020

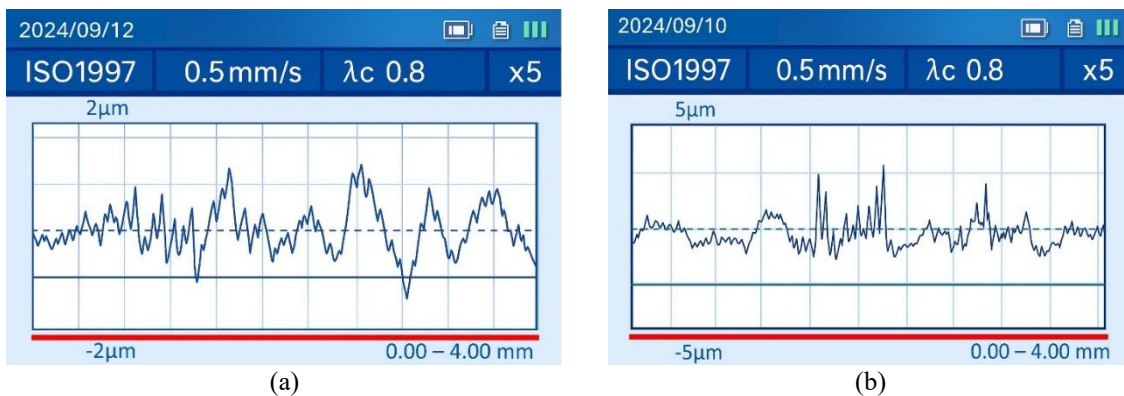


Figure 6. (a) Surface topography of the polygonal shaft model of AISI 304 material at CS 48 SPM and DoC 0.6 mm  
(b) Surface topography of the polygonal shaft model of AISI 1020 material at CS 48 SPM and DoC 0.6 mm

The surface roughness topography of the polygonal shaft models of AISI 304 (a) and AISI 1020 (b) materials is displayed in Figure 6 after turn-milling, with machining parameters of CS 48 SPM and DoC 0.6 mm for both materials. Peaks and valleys in graphs (a) and (b) represent surface roughness. The ISO 4287-1997 standard stylus-type contact method was used to make the measurements, which had a scanning stylus path length of 0–4 mm on the horizontal axis and a measurement speed of 0.5 mm/s. The surface roughness fluctuation pattern on the sharply spiked peaks and valleys is pretty noticeable in Figure 6(a).

More than half of the measurement path shows the sharp peaks and valleys. Using the measurement technique shown in Figure 3(b), the surface roughness is determined from the middle to the end of the workpiece. A topographic graphic

display for AISI 1020 is shown in Figure 6(b), which features notable peaks and valleys in the middle of the polygonal axis. High surface roughness is generally indicated by a significant difference between the prominent (peaks) and concave (valleys) portions of the surface. On the other hand, a smoother and flatter surface is characterized by a fluctuation pattern of peaks and valleys that tends to be gentle, with gradual changes.

**3.2 Statistical Analysis of Dimension Error (DE)**

The cutting speed (A) and depth of cut (B) variables did not significantly affect the dimensional error of the machined parts, according to the RSM analysis. Neither of the input variables in the tested range is strong enough to significantly affect the dimension error response, as indicated by the P-value > 0.05 in Table 6. In the test range, input parameters A and B result in dimensional failure (dimension error) that is reasonably stable (Figure 7(a) and (b)). This means that changes in input parameters do not significantly alter the dimension error response.

Table 6. ANOVA for Mean Model (response: Dimension error in mm)

Source	Sum of Squares	df	Mean Square	F-value	p-value	
<b>AISI 304</b>						
Model	0.0000	0				
Residual	0.0199	17	0.0012			
Lack of Fit	0.0098	8	0.0012	1.10	0.4429	not significant
Pure Error	0.0101	9	0.0011			
Cor Total	0.0199	17				
Standard Deviation	0.0342		R <sup>2</sup>	0.0000		
Mean	-0.0220		Adjusted R <sup>2</sup>	0.0000		
C.V. %	155.37		Predicted R <sup>2</sup>	-0.1211		
PRESS	0.0223		Adeq. Precision	NA <sup>(1)</sup>		
<b>AISI 1020</b>						
Model	0.0000	0				
Residual	0.0419	17	0.0025			
Lack of Fit	0.0207	8	0.0026	1.10	0.4412	
Pure Error	0.0212	9	0.0024			
Cor Total	0.0419	17				
Standard Deviation	0.0497		R <sup>2</sup>	0.0000		
Mean	-0.0417		Adjusted R <sup>2</sup>	0.0000		
C.V. %	119.12		Predicted R <sup>2</sup>	-0.1211		
PRESS	0.0470		Adeq. Precision	NA <sup>(1)</sup>		

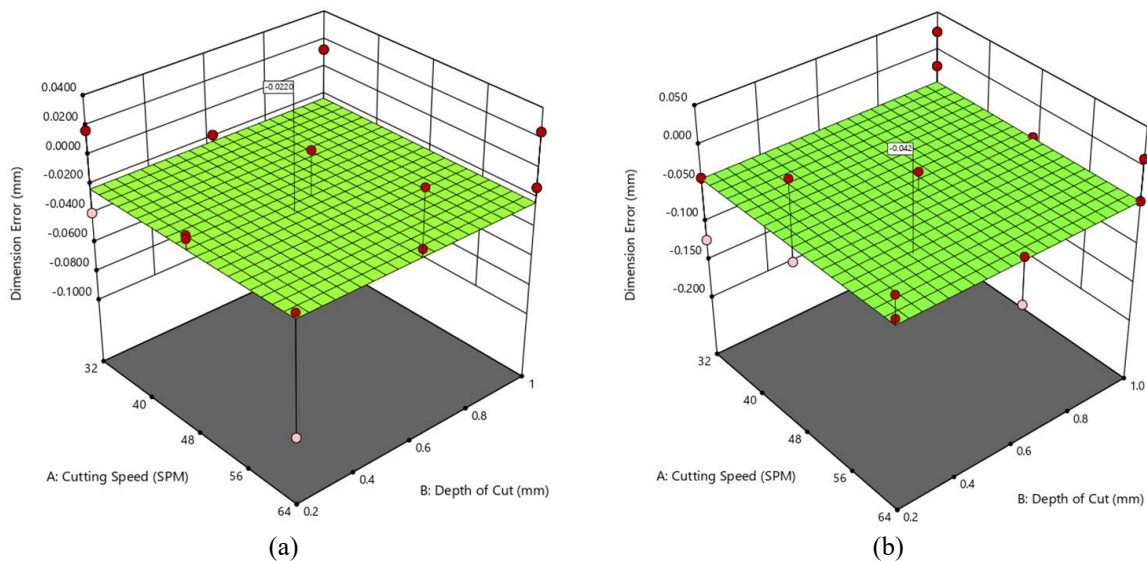


Figure 7. 3D response surface plot for dimension error of AISI 304 (a) and AISI 1020 (b)

According to Nisar et al [23], the feed rate parameter is the most important factor influencing dimensional accuracy. Islam et al. [55] explained that the cooling method has a moderate contribution to dimensional accuracy in the titanium turning process. This investigation was carried out experimentally and analytically. Test data were analyzed using three methods, namely traditional analysis, Pareto ANOVA, and the Taguchi method. Other research on dimensional accuracy was conducted by Villarrazo et al. [56] on the ball-end milling of thin-walled blades. This research focuses on the effect of tool orientation on surface roughness and dimensional accuracy of Ti6Al4V material. Four inclination angles (15°, 30°, 45°, and 60°) were used in the test, and the results showed that inclination angle significantly affected surface quality and dimensional precision. The 30° inclination angle provided the best balance between surface finish and dimensional tolerance. Other potential causes include a parameter range that is too narrow or other machining factors such as feed rate, material type, and vibration.

### 3.3 Statistical Analysis of Time Cycle (TC)

Table 7 summarizes the ANOVA results for the time-cycle response. The p-values for both input variables (A) and (B) are less than 0.05 ( $<0.0001$ ), indicating that they have a significant impact on the response. The variable that most significantly affects the reaction in AISI 304 material is depth of cut (B), with an F-value of 119.54. Cutting speed (A) comes in second with a 34.12, quadratic (B) with a 26.92, and the interaction between (A) and (B) with a 24.68. In the AISI 1020 material, the response variable is significantly impacted by the quadratic term, as well as the interaction between all input variables (A) and (B).

The input variable with the most significant impact on the response is depth of cut (B), with an F-value of 492.73. Cutting speed (A), quadratic (B), interaction (A) and (B), and quadratic (A) have F-values of 105.05, 71.30, 41.64, and 8.17, respectively. The predicted  $R^2$  and adjusted  $R^2$  values of 0.8808 and 0.9231 for AISI 304 material, and 0.9638 and 0.9767 for AISI 1020 material, respectively, demonstrate the quality of the statistical model.

Table 7. ANOVA for response quadratic model (response: Time Cycle in minutes)

Source	Sum of Squares	df	Mean Square	F-value	p-value	
AISI 304						
Model	543.55	5	108.71	41.84	$< 0.0001$	significant
Cutting Speed (A)	88.65	1	88.65	34.12	$< 0.0001$	
Depth of Cut (B)	310.59	1	310.59	119.54	$< 0.0001$	
AB	64.13	1	64.13	24.68	0.0003	
A <sup>2</sup>	10.22	1	10.22	3.93	0.0707	
B <sup>2</sup>	69.95	1	69.95	26.92	0.0002	
Residual	31.18	12	2.60			
Lack of Fit	30.97	3	10.32	440.95	$< 0.0001$	significant
Pure Error	0.2107	9	0.0234			
Cor Total	574.73	17				
Standard Deviation	1.61		R <sup>2</sup>	0.9457		
Mean	6.81		Adjusted R <sup>2</sup>	0.9231		
C.V. %	23.67		Predicted R <sup>2</sup>	0.8808		
PRESS	68.49		Adeq. Precision	18.8437		
AISI 1020						
Model	321.22	5	64.24	143.78	$< 0.0001$	significant
Cutting Speed (A)	46.94	1	46.94	105.05	$< 0.0001$	
Depth of Cut (B)	220.16	1	220.16	492.73	$< 0.0001$	
AB	18.60	1	18.60	41.64	$< 0.0001$	
A <sup>2</sup>	3.65	1	3.65	8.17	0.0144	
B <sup>2</sup>	31.86	1	31.86	71.30	$< 0.0001$	
Residual	5.36	12	0.4468			
Lack of Fit	5.36	3	1.79			
Pure Error	0.0000	9	0.0000			
Cor Total	326.58	17				
Standard Deviation	0.6685		R <sup>2</sup>	0.9836		
Mean	6.01		Adjusted R <sup>2</sup>	0.9767		
C.V. %	11.11		Predicted R <sup>2</sup>	0.9638		
PRESS	11.84		Adeq Precision	33.7496		

The time cycle response on AISI 304 and 1020 materials is predicted by Equations (4) and (5) using the two influencing variables. A negative value on each variable's coefficient in Eqs. (4) and (5) indicate that increasing variables

(A) and (B) each produce a decreasing time cycle response variable. Nevertheless, the interaction can raise the time cycle response value by raising both variables. The same is true of variable (B)'s quadratic.

$$\{TC(AISI\ 304) = 55.27940 - 1.03479 \cdot CS - 65.31771 \cdot DoC + 0.442383 \cdot CS \cdot DoC + 0.006245 \cdot CS^2 + 26.13715 \cdot DoC^2\} R^2 = 94.57\%, R_{Adj}^2 = 92.31\% \tag{4}$$

$$\{TC(AISI\ 1020) = 37.66713 - 0.624913 \cdot CS - 43.31250 \cdot DoC + 0.238281 \cdot CS \cdot DoC + 0.003733 \cdot CS^2 + 17.63889 \cdot DoC^2\} R^2 = 98.36\%, R_{Adj}^2 = 97.67\% \tag{5}$$

In a machining process, efficiency concerns are crucial. Efficiency naturally increases when a machining process takes less time, as this has a significant impact on production costs. Without considering the product's quality or preventing machine damage, this machining time cannot be justified on its own. To achieve this, machining parameters are optimized. The graphic representation of the relationship between cutting speed, depth of cut variables and the time cycle response is shown in Figure 8. Cutting speed, depth of cut, and time cycle response are just a few of the input and response variables that are described by each axis on the graph.

As shown in Figures 8 (a) and (b), the combination of decreasing the cutter's speed (A) and decreasing the depth of cut (B) results in an increase in cycle time for the machining process on both materials. According to the blue area graph, a shorter machining time can be achieved by combining variables (A) 48-64 SPM and (B) 0.8-1 mm. Optimization of the machining time based on the interaction of input variables determined ideal machining times of 3.96 minutes and 5 minutes for each material. The surface quality of the machined workpiece must also be considered in relation to this time optimization.

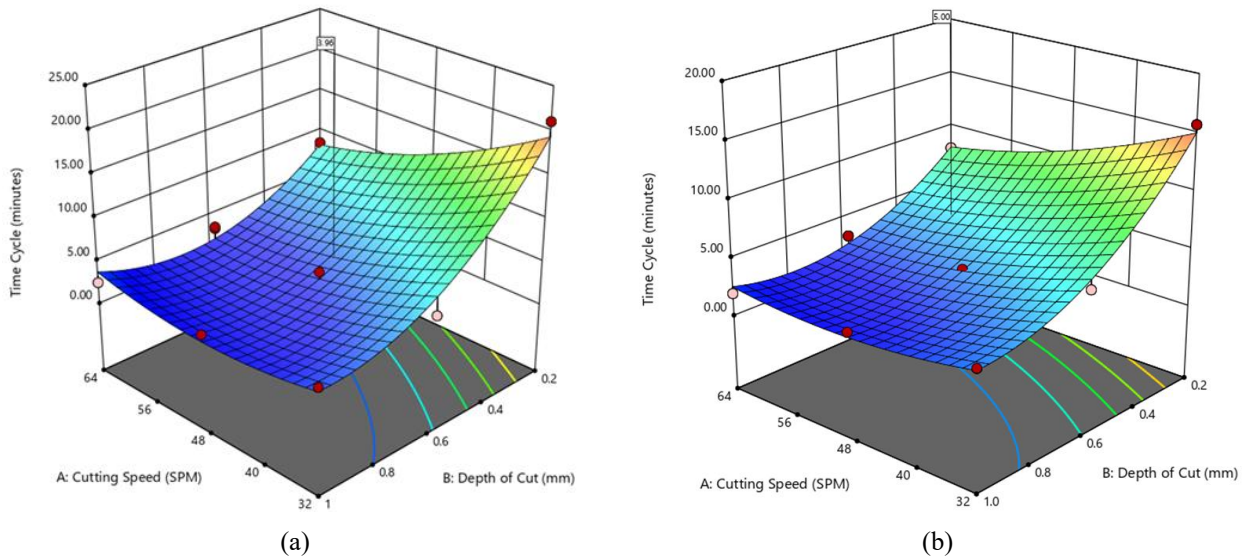


Figure 8. 3D response surface plot for the time cycle of (a) AISI 304 and (b) AISI 1020 (b)

#### 4. CONCLUSIONS

This paper presents the optimization of the turn-milling machining process for manufacturing polygonal shaft models from AISI 304 and 1020 materials, employing the response surface methodology (RSM). The machining parameters for the input variables used in this machining process are cutting speed (A) and depth of cut (B), where both of these variables are varied to see their effect on the output/response variables in the form of machining results quality, which includes surface roughness and dimension error, as well as machining time efficiency in the form of time cycle in a machining test. According to the results of the optimization process using a CNC turn-milling machine, the depth of cut parameter has the greatest influence on the workpiece's surface roughness and cycle time, but has a minimal effect on dimensional error.

According to the ANOVA results for the quadratic response model, the input variables have a significant impact on the materials' surface roughness and time cycle, as indicated by the p-value < 0.05. The predicted R<sup>2</sup> value for surface roughness is 0.7756, the adjusted R<sup>2</sup> value is 0.8538 for AISI 304, and the predicted R<sup>2</sup> is 0.6443, and the Adjusted R<sup>2</sup> is 0.7771 for AISI 1020. For AISI 304 and AISI 1020 materials, the predicted R<sup>2</sup> and adjusted R<sup>2</sup> values for the time cycle are 0.8808 and 0.9231, respectively, and 0.9638 and 0.9767. AISI 304 material yields the best surface roughness value of 0.3637µm at a cutting speed of 48 SPM and a depth of cut of 0.6 mm, while 1020 material yields 0.4045 µm at a cutting speed and depth of cut of 48 SPM and 0.6 mm. In contrast, 3.96 minutes and 5 minutes are the ideal machining times found for each material.

This experiment focused on the effects of cutting speed and depth of cut parameters in relation to machining quality. Therefore, it is highly recommended to conduct additional machining experiments to investigate the effects of feed rate, tool geometry, and vibration, as well as to analyze tribological aspects, including wear, friction, and lubrication.

## ACKNOWLEDGEMENTS

The authors thank the National Research and Innovation Agency for providing laboratory support and funding for this research activity.

## CONFLICT OF INTEREST

The authors declare that they have no conflicts of interest or personal relationships that could have influenced the work presented in this paper.

## AUTHORS' CONTRIBUTION

U. Hanifah: Writing – original draft, formal analysis, funding acquisition, project administration.

Novrinaldi: Writing – original draft, conceptualization, methodology, formal analysis, data curation, investigation, supervision.

M. Andrianto, S. A. Putra, A. Haryanto, A. Taufan, M. Furqon, E. K. Pramono, Y. H. Siregar, D. Sagita: Writing – review & editing, investigation.

Ma'muri, M. Azka: Writing – review & editing.

N. A. Rofik, S. Rhamadhan: Investigation.

## REFERENCES

- [1] W. Li and Q. Yan, "Failure analysis of an isometric polygonal shaft fracture," *Engineering Failure Analysis*, vol. 58, pp. 192–205, 2015.
- [2] T. Arndt, V. Sellmeier, and V. Schulze, "Model-based tool design for the manufacturing of hypocycloidal internal profiles by polygon turning," *Procedia CIRP*, vol. 117, pp. 7–12, 2023.
- [3] L. Liu, W. Jia, D. Xu, and R. Li, "A profile shaft connection technique and its applications in transmission structure," *International Journal of Manufacturing Technology and Management*, vol. 28, no. 4, pp. 336–348, 2014.
- [4] B. Lü and K. Liu, "Research on stress and strain in isometric polygonal profile connection based on FEM," *Key Engineering Materials*, vol. 460–461, pp. 369–373, 2011.
- [5] D. S. Wang, A. P. Zhou, and Y. L. Yuan, "Study of a CNC grinding machining method using an isometric polygon profile," *Journal of Materials Processing Technology*, vol. 129, no. 1–3, pp. 237–240, 2002.
- [6] D. S. Wang, A. P. Zhou, P. L. Huang, and X. Y. Zhao, "Time series model study on the NC grinding process of isometric polygonal profile," *Materials Science Forum*, vol. 471–472, pp. 518–522, 2004.
- [7] D. Wang, A. Zhou, and Y. Zhao, "Research on NC grinding accessories of Isometric Polygonal Profile," *Key Engineering Materials*, vol. 416, pp. 93–97, 2009.
- [8] O. Szabó, "Application and modelling of polygon joints torque transmissions in the power transmission of electromobiles," *IoP Conference Series: Materials Science and Engineering*, vol. 448, no. 1, 2018.
- [9] J. T. Maximov, "A new method of manufacture of hypocycloidal polygon shaft joints," *Journal of Materials Processing Technology*, vol. 166, no. 1, pp. 144–149, 2005.
- [10] E. Soliman, "Simulation of the polygonal turning process," *Journal of Manufacturing Processes*, vol. 80, no. May, pp. 852–859, 2022.
- [11] M. Regus, A. Patalas, R. Łabudzki, F. Sarbinowski, and R. Talar, "Studies of polygons accuracy shaped by various methods on universal CNC turning center," *IOP Conference Series: Materials Science and Engineering*, vol. 393, no. 1, 2018.
- [12] D. A. Stephenson and J. S. Agapiou, *Metal cutting theory and practice*, 3<sup>rd</sup> edition. New York: CRC Press, 2016.
- [13] V.-L. Trinh, "A review of the surface roughness prediction methods in finishing machining," *Engineering, Technology & Applied Science Research*, vol. 14, no. 4 SE-, pp. 15297–15304, 2024.
- [14] R. Liu and W. Tian, "A novel simultaneous monitoring method for surface roughness and tool wear in milling process," *Scientific Reports*, vol. 15, no. 1, pp. 1–11, 2025.
- [15] C. Felho, B. Karpuschewski, and J. Kundrák, "Surface roughness modelling in face milling," *Procedia CIRP*, vol. 31, pp. 136–141, 2015.
- [16] S. Roy, R. Kumar, A. K. Sahoo, and A. Panda, "Cutting tool failure and surface finish analysis in pulsating MQL-assisted hard turning," *Journal of Failure Analysis and Prevention*, vol. 20, no. 4, pp. 1274–1291, 2020.
- [17] Anurag, R. Kumar, A. K. Sahoo, and A. Panda, "Comparative performance analysis of coated carbide insert in turning of Ti-6Al-4V ELI grade alloy under dry, minimum quantity lubrication and spray impingement cooling environments," *Journal of Materials Engineering and Performance*, vol. 31, no. 1, pp. 709–732, 2022.

- [18] M. S. Najiha, M. M. Rahman, and K. Kadirgama, "Parametric optimization of end milling process under minimum quantity lubrication with nanofluid as cutting medium using Pareto optimality approach," *International Journal of Automotive and Mechanical Engineering*, vol. 13, no. 2, pp. 3345–3360, 2016.
- [19] C. Li, G. Zhao, D. Ji, G. Zhang, L. Liu, F. Zeng, et al., "Influence of tool wear and workpiece diameter on surface quality and prediction of surface roughness in turning," *Metals (Basel)*, vol. 14, no. 11, 2024.
- [20] G. Kumar, M. Atif Wahid, P. Tanwar, and M. Kumar, "Multi performance characteristics optimization of end milling parameters on surface quality and Micro-hardness of SS-304," *Materials Today: Proceedings*, vol. 62, pp. 136–141, 2022.
- [21] N. Verma, M. Sarkar, R. K. Gautam, S. Rathore, K. Laiq, and A. Khan, "Optimisation of machining parameters for CNC milling of magnesium alloy AZ91 by using the Taguchi technique," *Tuijin Jishu/Journal of Propulsion Technology*, vol. 44, no. 4, pp. 680–695, 2023.
- [22] R. Mahesh, Thakur Paramjit and Rajesh, "Optimal selection of process parameters in CNC end milling of Al 7075-T16 aluminium alloy using a Taguchi-Fuzzy approach," in *International Conference on Advances in Manufacturing and Materials Engineering, AMME 2014*, ScienceDirect Elsevier, 2014, pp. 2493–2502.
- [23] L. Nisar, B. Banday, M. Amatullah, M. Farooq, A. N. Thoker, A. Maqbool, et al., "An investigation on effect of process parameters on surface roughness and dimensional inaccuracy using Grey based Taguchi method," *Materials Today: Proceedings*, vol. 46, pp. 6564–6569, 2020.
- [24] M. Villeta, E. M. Rubio, J. M. Sáenz De Pipaón, and M. A. Sebastián, "Surface finish optimization of magnesium pieces obtained by dry turning based on Taguchi techniques and statistical tests," *Materials and Manufacturing Processes*, vol. 26, no. 12, pp. 1503–1510, 2011.
- [25] R. Kumar, G. Krishna M, E. Billu, A. K. Reddy D, and S. Ram, "Optimization of surface roughness in machining of titanium composite using Taguchi method," *Interactions*, vol. 246, no. 1, p. 33, 2025.
- [26] M. Ayyıldız, "Optimization and prediction of surface roughness in the milling process of aluminum alloy using Taguchi method and artificial neural network," *Multidiscipline Modeling in Materials and Structures*, vol. 21, no. 5, pp. 1204–1216, 2025.
- [27] M. Sarikaya and A. Güllü, "Taguchi design and response surface methodology based analysis of machining parameters in CNC turning under MQL," *Journal of Cleaner Production*, vol. 65, pp. 604–616, 2014.
- [28] S. M. Kumar, "Investigation of surface roughness and material removal rate for UD-GFRP composite using Taguchi grey relational analysis," *International Journal of Automotive and Mechanical Engineering*, vol. 14, no. 2, pp. 4298–4314, 2017.
- [29] T. Singh, J. S. Dureja, M. Dogra, and M. S. Bhatti, "Machining performance investigation of AISI 304 austenitic stainless steel under different turning environments," *International Journal of Automotive and Mechanical Engineering*, vol. 15, no. 4, pp. 5837–5862, 2018.
- [30] V. Mugendiran, A. Gnanavelbabu, and R. Ramadoss, "Parameter optimization for surface roughness and wall thickness on AA5052 Aluminium alloy by incremental forming using response surface methodology," *Procedia Engineering*, vol. 97, pp. 1991–2000, 2014.
- [31] R. Roy, M. Islam, M. J. Shazida, R. K. Mollik, and M. Billah, "Optimization of process parameters in CNC end milling of mild steel using optimization of process parameters in CNC end milling of mild steel using response surface methodology," in *7th Bangladesh Conference on Industrial Engineering and Operations Management December 21-22, 2024*, 2024, p. 357.
- [32] J. C. Puoza, T. Zhang, F. Uba, Y. Kuusana, and A. Ibrahim, "Experimental optimization of high-precision turning parameters of AL6061 materials for automotive industry based on grey relational analysis," *International Journal of Automotive and Mechanical Engineering*, vol. 20, no. 4, pp. 10878–10893, 2023.
- [33] *Properties and selection: Irons steels and high performance alloys*, 10<sup>th</sup> Edition, ASM International Handbook Committee, 1993. [online] ASM Metals Handbook, Vol 09.pdf - Google Drive
- [34] A. Pramanik, H. Sanghvi, and A. K. Basak, "Object-based final-year project: Designing and manufacturing a quick stop device," in *Modern Manufacturing Engineering*, J. Paulo Davim, Ed., pp. 271–299, 2015. Springer Cham.
- [35] M. P. Groover, "Part II Engineering Materials," in *Fundamentals of Modern Manufacturing*, pp. 98–132, 2010.
- [36] I. S. Jawahir, J. Schoop, Y. Kaynak, A. K. Balaji, R. Ghosh, and T. Lu, "Progress toward modeling and optimization of sustainable machining processes," *Journal of Manufacturing Science and Engineering*, vol. 142, no. 11, 2020.
- [37] M. F. Rajemi, P. T. Mativenga, and A. Aramcharoen, "Sustainable machining: Selection of optimum turning conditions based on minimum energy considerations," *Journal of Cleaner Production*, vol. 18, no. 10–11, pp. 1059–1065, 2010.
- [38] D. Y. Pimenov, M. Mia, M. K. Gupta, Á. R. Machado, G. Pintaude, D. R. Unune, et al., "Resource saving by optimization and machining environments for sustainable manufacturing: A review and future prospects," *Renewable and Sustainable Energy Reviews*, vol. 166, p. 112660, 2022.
- [39] J. V. Abellán-Nebot, C. Vila Pastor, and H. R. Siller, "A review of the factors influencing surface roughness in machining and their impact on sustainability," *Sustainability*, vol. 16, no. 5, p. 1917, 2024.
- [40] *ISO 3274:1996 Geometrical Product Specifications (GPS) — Surface texture: Profile method — Nominal characteristics of contact (stylus) instruments, 61010-1* © Iec2001, International Organization for Standardization, Edition 2, 1996.
- [41] *ISO 11402:2004: Phenolic, amino and condensation resins — Determination of free-formaldehyde content*, International Organization for Standardization, Edition 2, 2004.
- [42] A. Mahyar Khorasani, M. Reza Soleymani Yazdi, and M. S. Safizadeh, "Analysis of machining parameters effects on surface roughness: A review," *International Journal of Computational Materials Science and Surface Engineering*, vol. 5, no. 1, pp. 68–84, 2012.

- [43] Y. Abidi and L. Boulanouar, "Correlation analysis between tool wear, roughness and cutting vibration in turning of hardened steel," *Engineering Transactions*, vol. 69, no. 4, pp. 403–421, 2021.
- [44] G. Bartarya and S. K. Choudhury, "Effect of cutting parameters on cutting force and surface roughness during finish hard turning AISI52100 grade steel," *Procedia CIRP*, vol. 1, pp. 651–656, 2012.
- [45] M. Cao, C. Zhou, and K. M. Li, "Research on the relationship between workpiece surface machining quality and turning tool wear," *Journal of Physics: Conference Series*, vol. 2029, no. 1, p. 012071, 2021.
- [46] W. D. Lestari, R. Ismail, J. Jamari, A. P. Bayuseno, and P. W. Anggoro, "Optimization of CNC milling parameters through the Taguchi and RSM methods for surface roughness of UHMWPE acetabular cup" *International Journal of Mechanical Engineering and Technology*, vol. 10, no. 2, pp. 1762–1775, 2019.
- [47] A. Aziz, M. Azka, A. Susanto, K. Jauhari, and R. Nurmayni, "Influence of Lubrication on Vibration Response and Surface Roughness in Milling of Aluminum 6061," *Evergreen*, vol. 10, no. 3, pp. 1762–1769, 2023.
- [48] W. Zhong, D. Zhao, and X. Wang, "A comparative study on dry milling and little quantity lubricant milling based on vibration signals," *International Journal of Machine Tools and Manufacture*, vol. 50, no. 12, pp. 1057–1064, 2010.
- [49] I. Zagorski, A. Weremczuk, M. Kulisz, and A. Skoczylas, "Vibration and stability in dry rough milling AZ31B magnesium alloy using end mills with different edge geometry," *Measurement*, vol. 256, part E, p. 118523, 2025.
- [50] R. Chaari, M. Haddar, F. Djemal, F. Chaari, and M. Haddar, "Passive vibration absorber effect on the machining surface quality of a flexible workpiece," *Comptes Rendus. Mécanique*, vol. 347, no. 12, pp. 903–911, 2019.
- [51] L. Xin, "Research on tool wear and prediction of machined surface roughness during machining of H13 steel," Shandong University, 2020.
- [52] M. Kuttolamadom, S. Hamzehlouia, and L. Mears, "Effect of machining feed on surface roughness in cutting 6061 aluminum," *SAE International Journal of Materials and Manufacturing*, vol. 3, no. 1, pp. 108–119, 2010.
- [53] D. Deepak and B. Rajendra, "Optimization of machining parameters for turning of Al6061 using robust design principle to minimize the surface roughness," *Procedia Technology*, vol. 24, pp. 372–378, 2016.
- [54] L. Hao, "Discussion on surface quality and precision control of metal materials in machining process," *Journal of Physics: Conference Series*, vol. 2174, no. 1, 2022.
- [55] M. N. Islam, J. M. Anggono, A. Pramanik, and B. Boswell, "Effect of cooling methods on dimensional accuracy and surface finish of a turned titanium part," *The International Journal of Advanced Manufacturing Technology*, vol. 69, no. 9–12, pp. 2711–2722, 2013.
- [56] N. Villarrazo, Á. Sáinz de la Maza, S. Caneda, L. Bai, O. Pereira, and L. N. López de Lacalle, "Effect of tool orientation on surface roughness and dimensional accuracy in ball end milling of thin-walled blades," *The International Journal of Advanced Manufacturing Technology*, vol. 136, no. 1, pp. 383–395, 2025.